nature communications

Article

https://doi.org/10.1038/s41467-024-54051-1

Photosynthetic directed endosymbiosis to investigate the role of bioenergetics in chloroplast function and evolution

Received: 7 November 2023

Accepted: 30 October 2024

Published online: 10 December 2024

Check for updates

Bidhan Chandra De[1], Jay Cournoyer[1], Yang-le Gao[1], Catherine L. Wallace[2], Stanley Bram[1] & Angad P. Mehta[1,3,4]

Cyanobacterial photosynthesis (to produce ATP and NADPH) might have played a pivotal role in the endosymbiotic evolution to chloroplast. However, rather than meeting the ATP requirements of the host cell, the modern-day land plant chloroplasts are suggested to utilize photosynthesized ATP predominantly for carbon assimilation. This is further highlighted by the fact that the plastidic ADP/ATP carrier translocases from land plants preferentially import ATP. Here, we investigate the preferences of plastidic ADP/ATP carrier translocases from key lineages of photosynthetic eukaryotes including red algae, glaucophytes, and land plants. Particularly, we observe that the cyanobacterial endosymbionts expressing plastidic ADP/ATP carrier translocases from red algae and glaucophyte are able to export ATP and support ATP dependent endosymbiosis, whereas those expressing ADP/ATP carrier translocases from land plants preferentially import ATP and are unable to support ATP dependent endosymbiosis. These data are consistent with a scenario where the ancestral plastids may have exported ATP to support the bioenergetic functions of the host cell.

Chloroplasts evolved from cyanobacterial endosymbionts (symbionts within host cells) established within eukaryotic cells[1–5]. This key evolutionary event was foundational to the evolution of photosynthetic eukaryotic life forms, including plants. Modern-day chloroplasts perform various functions like carbon assimilation, sulfate assimilation, nitrate assimilation, amino acid biosynthesis, fatty acid biosynthesis amongst others[4]. However, it is unclear what the exact functions of the early cyanobacterial endosymbionts were. Indirect insights have been obtained from host and organelle genome sequencing, bioinformatics analysis, and investigations into chloroplast biochemistry. Particularly, these studies have helped to identify the features retained within the organelles, metabolic pathways that were redundant and lost from the organelle genome, and pathways and adaptation elements that were transferred from the endosymbiont genome to the host genome. Despite all these studies, the key drivers of the endosymbiotic evolution of chloroplast are still unclear[6]. It is widely suggested that in the case of chloroplast evolution, the cyanobacterial oxygenic photosynthesis to produce ATP and NADPH may have been one of the key drivers[6–8]. This is highlighted by the fact that ADP/ATP carrier translocases and transporters are widely conserved across organelles like mitochondria and chloroplasts, including organisms that are related to the endosymbiotic precursors of mitochondria and chloroplasts[9,10].

ADP/ATP carrier translocases localized on the membrane of organelles facilitate the exchange of ATP and ADP between the cytoplasm and the organelle; this feature is crucial for the organelle to perform key bioenergetic functions for the host cell. The preference for ATP export versus ATP import is suggested to vary from one organelle to other. Importantly, the preferences of ATP import versus

[1]Department of Chemistry, University of Illinois at Urbana-Champaign, 600 S Mathews Avenue, Urbana, IL, US. [2]The Imaging Technology Group, Beckman Institute for Advanced Science & Technology, University of Illinois at Urbana-Champaign, 405 North Mathews Avenue, Urbana, IL, US. [3]Carl R. Woese Institute for Genomic Biology, University of Illinois at Urbana-Champaign, 1206 West Gregory Drive, Urbana, IL, US. [4]Cancer Center at Illinois, University of Illinois at Urbana-Champaign, 405 North Mathews Avenue, Urbana, IL, US. e-mail: apm8@illinois.edu

export for mitochondrial versus plastidic ADP/ATP carrier translocases reflect the roles of the organelles[8,9,11,12]. Briefly, it is generally accepted that the key function of modern-day land plant chloroplasts is carbon assimilation. On the other hand, the mitochondria within the land plant cells provide ATP (generated from oxidative phosphorylation) to the host cell while the chloroplasts utilize photosynthesized ATP predominantly for carbon assimilation instead of supplying it to the host cell[13]. Therefore, unlike the mitochondrial ADP/ATP carrier translocases that preferentially export ATP, the ADP/ATP carrier translocases from the plastids of green land plants preferentially import ATP[9,12]. The major ATP burden of the land plant cells is supported by mitochondrial oxidative phosphorylation, and this is highlighted by the fact that mitochondrial ADP/ATP carrier translocases preferentially export ATP[13]. However, it is important to note that the chloroplasts still play an important role in cellular bioenergetics by contributing assimilated carbon sources. In contrast, the major function of the endosymbiont that was the key precursor of chloroplast is unclear; particularly it is unclear if the cyanobacterial endosymbionts also provided photosynthetically generated ATP in addition to assimilated carbon. We hypothesized that studying the preferences of plastidic ATP/ADP carrier proteins from various lineages of photosynthetic eukaryotes, i.e., red algae, glaucophytes, and land plants, could provide some insights into the evolution of chloroplast functions[14]. Red algae are typically aquatic photoautotrophs[15,16]. Red algae belong to Archaeplastida and form a clade with land plants and glaucophyte algae[17]. Further red algal plastids have compacted and gene-rich architectures that most closely resemble the plastid ancestors, lack of unique unknown ORFs, highly conserved gene order, and slower rate of plastid-to-nucleus gene transfer amongst others[17,18]. Glaucophytes plastids share several traits with free-living cyanobacteria like peptidoglycan wall between the organelle membranes[19], similar composition of their photosynthetic apparatuses[20]. These molecular features are suggested to support the hypothesis that glaucophytes diverged earliest within Archaeplastida[21,22].

In this study, we bioinformatically identify putative ADP/ATP carrier translocases from red algae, glaucophytes and land plants. We then generate a series of cyanobacterial mutants that heterologously express these proteins for biochemical characterization using cyanobacterial cell-based assays (Fig. 1A). Next, using synthetic directed endosymbiosis (where the yeast cells depend on cyanobacterial endosymbionts for ATP)[23,24], we test whether the engineered cyanobacterial endosymbionts expressing these ADP/ATP carrier proteins are able to support the bioenergetic functions of the host yeast mutants that depend on these cyanobacterial endosymbionts for photosynthetically generated ATP (Fig. 1B). Particularly, we observe that the cyanobacterial endosymbionts expressing the ADP/ATP carrier translocases from red algae and glaucophytes are able to support photosynthesis-driven ATP-dependent endosymbiosis, whereas those expressing ADP/ATP carrier translocases from land plant plastids are unable to support photosynthesis-driven ATP-dependent endosymbiosis. These studies suggest that the chloroplast functions may have evolved over the course of evolution. Our investigations also result in the identification of a series of cyanobacterial mutants as optimal photosynthetic endosymbionts within yeast cells. We anticipate that such artificial photosynthetic yeast/cyanobacteria chimeras could also have the potential to be further developed for sustainable synthetic biology applications (e.g., photosynthetic metabolic engineering, carbon dioxide sequestration)[25].

Results

Identification of putative plastidic ADP/ATP carrier translocases

ATP acts as a universal cellular energy currency and is necessary for organelle function[26]. Membrane proteins that transport ADP and ATP have been identified in mitochondria, plastids, and obligate intracellular parasites. In plants, nucleotides are carried through via translocase proteins, adenine nucleotide uniporter, a subclass of functionally diverse mitochondrial carrier family (MCF) proteins and plastidic nucleotide transporter proteins[26,27]. The plastidic nucleotide transporter proteins are structurally and phylogenetically different from mitochondrial carrier family (MCF)-type carriers but are related to functionally heterogeneous ADP/ATP carrier translocases from obligate intracellular bacteria[11,28–30]. In an effort to identify non-mitochondrial ADP/ATP carrier translocase encoding genes, we bioinformatically analyzed the genomic data using the NCBI non-redundant database, a Position-Specific Iterative Basic Local Alignment Search Tool (PSI-BLASTP). To restrict our data set to include only AAC translocase proteins that can exchange ATP for ADP, we used the nucleotide transport protein (NTT) sequence NCBI id CAE46506.1 (https://www.ncbi.nlm.nih.gov/protein/CAE46506.1/) from *Protochlamydia ameoebophila* strain UWE25 as a query sequence for PSI-BLASTP analysis. This protein has been previously biochemically characterized in *Escherichia coli* and *Synechococcus elongatus PCC7942* (Syn7942) and has been demonstrated to facilitate ADP/ATP exchange[23,30]. Upon PSI-BLASTP search, we generated a comprehensive, non-redundant list of putative translocase protein sequences deposited in GenBank. The search protocol was restricted to organism-specific databases, for example: red algae (taxid:2763) or higher plants (taxid:3193) using an expectation value threshold of 0.05 to filter out putative ADP/ATP carrier candidates relevant to chloroplast function. A curated data set of 1,010 sequences were subjected to sequence similarity network (SSN) analysis using the Enzyme Function Initiative Enzyme Similarity Tool (EFI-EST)[31,32], as it allowed us to analyze and visualize a large number of sequences and compare them to sequences from red algae.

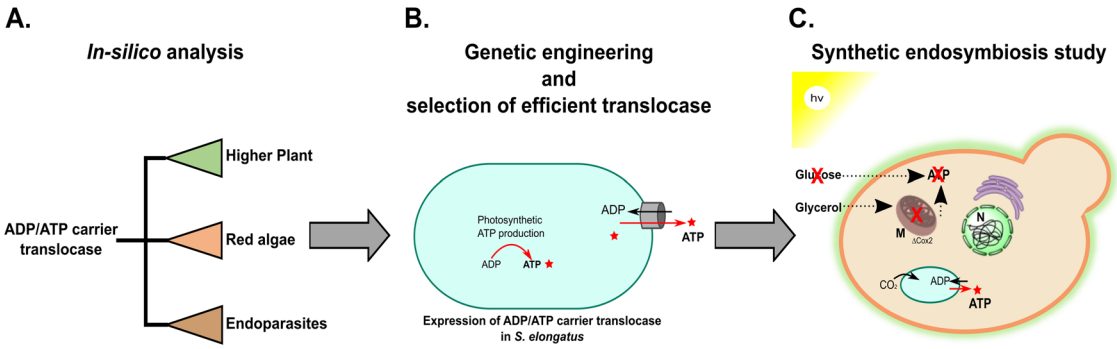

Fig. 1 | An approach to study the properties of plastidic ADP/ATP carrier translocases. A *In-silico* analysis and bioinformatic identification of plastidic ADP/ATP carrier translocase proteins from key lineages of photosynthetic eukaryotes. **B** Engineering cyanobacteria, *Synechococcus elongatus* PCC7942 (Syn7942), for recombinant expression of bioinformatically identification of plastidic ADP/ATP carrier translocase proteins. **C** ATP-dependent directed endosymbiosis between yeast mutants and cyanobacterial mutants expressing plastidic ADP/ATP carrier translocases.

https://doi.org/10.1038/s41467-024-54051-1

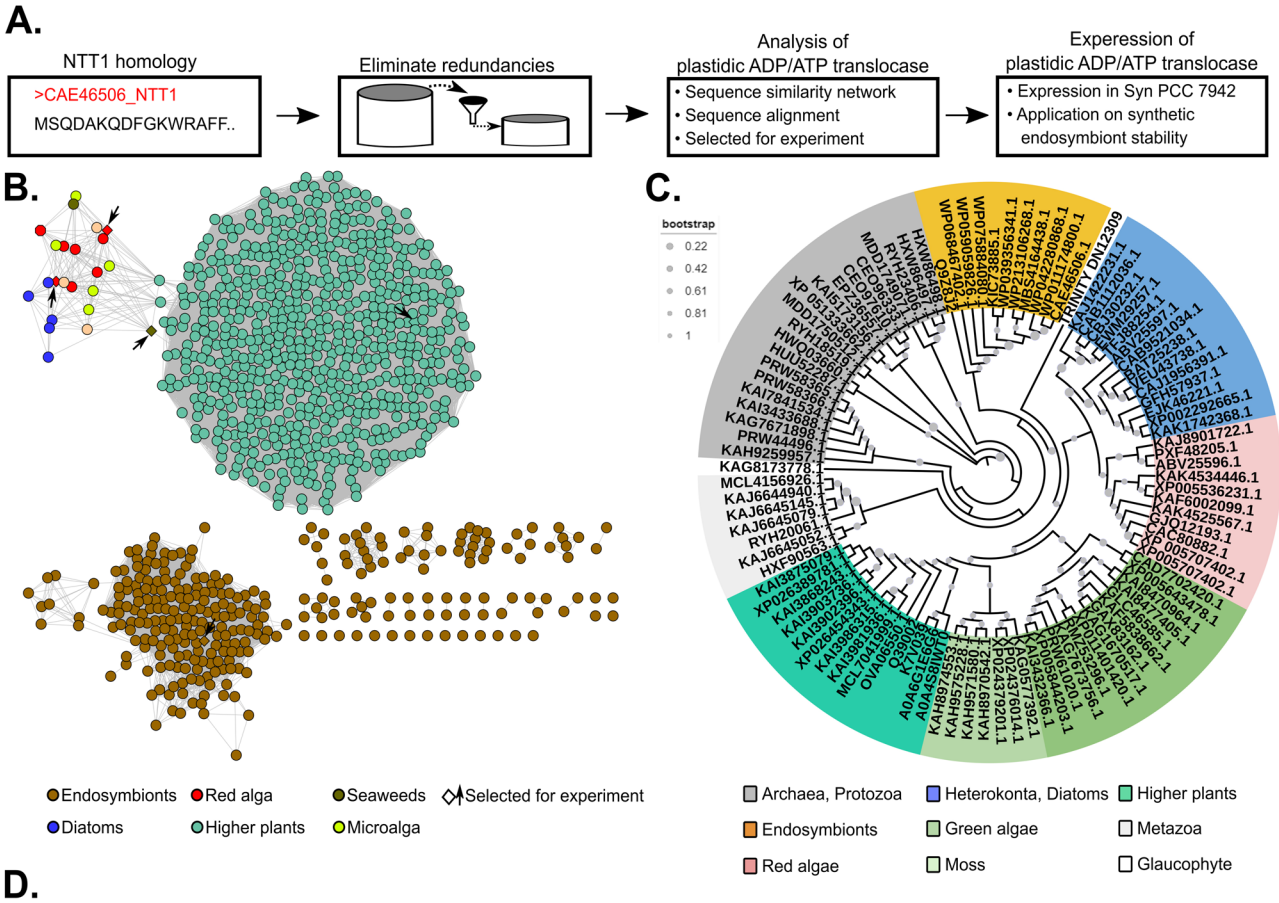

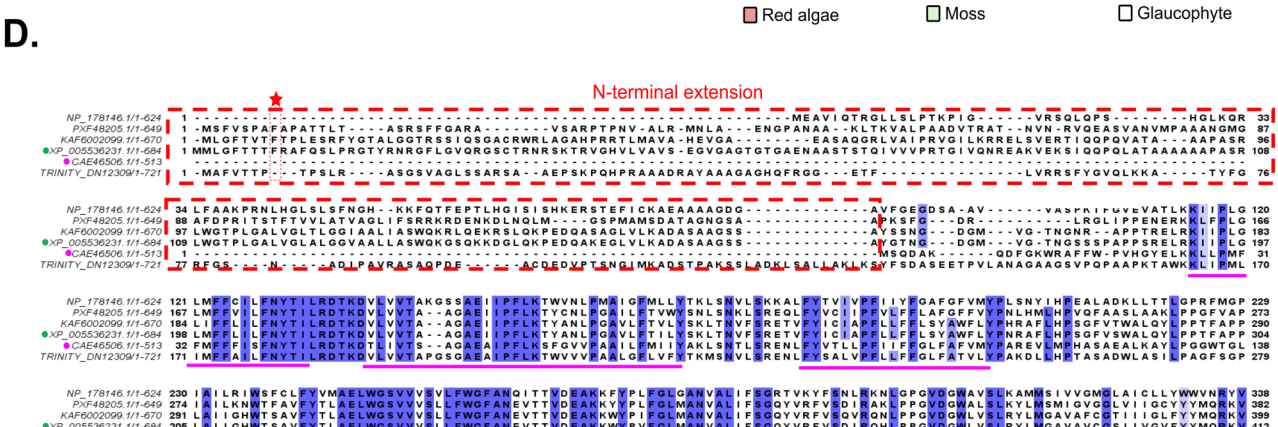

To examine the sequence diversity of the translocases and to classify them into different groups, SSNs for the ADP/ATP carrier translocase proteins were generated and presented using Cytoscape software (Fig. 2A)[33]. Among the 1,010 NCBI-identified AAC translocase genes, 500 genes belong to obligate intracellular parasites represented as group 1, with identity coverage of 90-100 %. The remaining 510 genes of red algae and/or higher plants are classified as group 2 with identity coverage of 50-60 %. Concentrating our analysis on ADP/ATP carrier translocases of plastidic origin, we selected a smaller subset of primary plastid ADP/ATP carrier sequences from each represented group, including a single available glaucophyte ADP/ATP carrier protein, for further analysis. These selections were based on the NCBI annotations identifying them as either of chloroplast origin or as hypothetical ADP/ATP carrier proteins. Subsequently, a phylogenetic tree was generated using Clustal Omega and MEGA X software. Furthermore, amino acid alignment and phylogenetic trees were

Fig. 2 | Bioinformatic analysis and identification of plastidic ADP/ATP carrier translocases. A The general workflow for identification and characterization of plastidic ADP/ATP carrier translocases. **B** Sequence similarity network (SSN) for ADP/ATP carrier translocase proteins found across the photosynthetic eukaryotes; the SSN is analyzed using an alignment score 120. The NTT proteins from Endosymbionts (Brown), and the ADP/ATP carrier translocase proteins from red algae (Red), diatoms (blue), microalgae/green algae (light green), higher plants (teal), the selected sequence from the SSN were presented rhombus border. **C** A smaller data set phylogenetic analysis of putative primary plastid ADP/ATP carrier translocase family proteins from archea to higher plant (see Results and Methods section). **D** Amino acid sequence alignment of selected NTT homologous and orthologs of putative plastidic ADP/ATP carrier translocase family protein from red algae and higher plant. The multiple sequence alignment was performed using Clustal Omega (https://www.ebi.ac.uk/Tools/msa/clustalo/) and data was presented using jalview software. Colored boxes indicate conserved amino acid residues among NTT and putative plastidic ADP/ATP carrier translocase family proteins from red algae and higher plant (100%: fore black, back blue; 80%–60%: fore black, back light blue). The pink dot represent amino acid query sequence: CAE46506.1; the Green dot amino acid sequence of plastidic putative ADP/ATP carrier protein (*Cyanidioschyzon merolae* strain 10D) NCBI id: XP_005536231.1 and its corresponding PDB id: M1V528; the dotted red rectangular box represented the N-terminal extension of putative plastidic ADP/ATP carrier translocase family proteins from red algae, glaucophyte and higher plant; the red star represented plastidic signal peptide conserved phenylalanine (F) essential organelle targeting; the pink underline represented the predicted twelve transmembrane domain for plastidic putative ADP/ATP carrier protein (*C. merolae* strain 10D) PDB id: M1V528. Source data are provided as a Source Data file.

constructed using the Maximum Likelihood statistical method (Fig. 2C, and Supplementary Fig. 1). Accompanying the SSN results, the phylogenetic tree showed a high co-occurrence of homologous ADP/ATP translocase genes specific to red algae and higher plants (Fig. 2B). We also performed phylogenetic analysis of the ADP/ATP carrier translocases (from obligate intracellular parasites and glaucophytes through red algae to higher plant, Fig. 2B, Supplementary Fig. 2)[8,34].

Using these analyses, we identified five putative ADP/ATP carrier genes, of NCBI id: *XP_005536231.1* (UniProt Primary accession: M1V528) gene from the red algal strain, *Cyanidioschyzon merolae* strain 10D of chloroplast carrier protein; *KAF6002099.1* gene from unicellular red algae *Cyanidiococcus yangmingshanensis* encoding a hypothetical carrier protein, *PXF48205.1* gene from *Gracilariopsis chorda* (a multicellular seaweed) of chloroplast origin; and *XP_005707402.1* gene from *Galdieria sulphuraria* (a unicellular extremophile red algae seaweed). Additionally, we also observed the presence of genes encoding hypothetical origin carrier protein, *CAX16542.1* and *TRINITY_DN12309* from, *Cyanophora paradoxa*, which are from a model glaucophyte species[21,35,36]. This search also resulted in the identification of a gene encoding uncharacterized non-mitochondrial ADP/ATP carrier translocase (UniProt Primary accession: Q39002), *NP_178146.1*, from *Arabidopsis thaliana;* given the similarity of this protein to the above putative red algal proteins, we decided to include this protein in our biochemical characterization efforts. These six genes encode proteins that have 55 to 57 % sequence identity to *P. ameoebophila* strain UWE25 nucleotide transport protein (NTT) (*CAE46506.1*). Additionally, an in silico localization analysis of these putative red algal ADP/ATP carrier translocases proteins found to contain stretches of N-terminal extended sequences with phenylalanine at the signal peptide cleavage site that resemble the "ASAFAP" motif of plastidic protein (Fig. 2C)[11]. We also compared the sequences of these putative proteins to the previously known and characterized ADP/ATP carrier translocase (*CAE46506.1*) of *Protochlamydia ameoebophila* strain UWE25 (UniProt accession: Q6MEM5), sequence alignments are shown in Fig. 2C. We also performed AlphaFold analysis of the putative ADP/ATP carrier translocases protein, M1V528, from red algae. The analysis predicted that the M1V528 protein could have 12 transmembrane domains (α-helices) (Fig. 2D, Supplementary Fig. 2 and Supplementary Fig. 3), similar to the *Protochlamydia* NTTs. This is consistent with the hypothesis that the plastidic translocases might have been acquired from *Chlamydiales* proteins like *Protochlamydia* NTTs[8,13]. There is limited characterization of these proteins as compared to the mitochondrial ATP/ADP carrier from the mitochondrial carrier family (MCF) protein subclass. To compare our studies on these translocases to another ADP/ATP carrier translocase protein from green land plant chloroplasts, we included previously identified thylakoid ATP/ADP carrier (NCBI id: NC_003076.8) from *Arabidopsis* which is not homologous to the above proteins but is suggested to be responsible for chloroplast ADP/ATP exchange[37]. This plastidic ADP/ATP carrier translocase protein from *Arabidopsis* was previously reported to preferentially import ATP and is suggested to supply nucleotides to the organelles[37]. A PSI-BLAST search in the NCBI data base also suggested proteins homologous to this plastidic ATP/ADP carrier translocase (NC_003076.8) from *Arabidopsis* were absent in red algae.

Engineering of Syn7942 mutant strains to recombinantly express ADP/ATP carrier translocases

Next, we experimentally tested several putative plastidic ADP/ATP carrier translocases identified above: XP_005536231.1, KAF6002099.1, PXF48205.1, XP_005707402.1 from red algae, NP_178146.1 from *A. thaliana* and NC_003076.8 (locus_tag=AT5G01500), a thylakoid ATP/ADP carrier. In order to biochemically characterize the putative ADP/ATP carrier proteins identified above, we engineered Syn7942 strains to heterologously express these proteins and used cell-based assays that we have previously developed to determine the biochemical properties of these proteins. Starting with a Syn7942 integrative plasmid pML17, we generated a series of plasmids (Supplementary Fig. 4 and Supplementary Data 1-2) allowing us to integrate a DNA cassette containing: (i) one of the defined AAC codon optimized sequences driven by a constitutive *pTrc* promoter; (ii) NSII integration site; (iii) chloramphenicol resistance marker; and (iv) genes encoding SNARE-like proteins (*Chlamydia trachomatis incA* and *CT_813*) that enhance the stability of yeast/cyanobacteria endosymbiosis[23,30,38]. Individual plasmids were transformed into Syn7942 and the transformants were selected on BG-11 medium containing chloramphenicol (10 μg/mL). The resistant colonies were repropagated, genomic DNA was isolated and the NSII site on the chromosome was tested for recombination using PCR analysis (Supplementary Figs. 5-6). Finally, we generated mutant strains SynBD1, SynBD2, SynBD3, SynBD4, SynBD6, SynBD7 and SynBD8 that possessed a genome-encoded copy of one of the translocases listed above (see Table 1 for more details). In addition to this, we also created a control strain SynBD5 that expresses the previously characterized *Arabidopsis* plastidic NTT gene. All these mutant strains were compared to wild-type Syn7942 and SynJEC3 strain expressing *Protochlamydia ameoebophila* strain UWE25 NTT protein (CAE46506.1) for their ability to exchange ADP and ATP.

Cell-based assays to biochemically characterize ADP/ATP carrier translocases

We next characterized if the putative ADP/ATP carrier translocases that were bioinformatically identified were functional when expressed in Syn7942 strains (Fig. 3A). Specifically, we first investigated the levels of ATP exported by each of the engineered mutants (listed in Fig. 3B) when challenged with extracellular ADP. We compared these levels to the levels of ATP exported when control strains SynJEC3 and Syn7942 were challenged with extracellular ADP. Luciferase assays were used for ATP detection. As expected, SynJEC3 strains exported significant levels of ATP when challenged with ADP compared to the wild-type Syn7942 strains. SynBD5 strains expressing non-mitochondrial ADP/ATP carrier translocase (NP_178146.1) were able

Table 1 | A list of cyanobacterial strains engineered, and corresponding integrative plasmid used in this study

Serial number	Strain designation	Suicide plasmid	Plasmid described	Genotype
1	SynJCE3	pML17	Cournoyer et al.[23]	*ΔNSII::CAT, Ptrac-UWE25-ntt1, Ctr-incA, CT_813*
2	SynBD1	pBD1	This study	*ΔNSII::CAT, Ptrac- XP_005536231.1, Ctr-incA, CT_813*
3	SynBD2	pBD2	This study	*ΔNSII::CAT, Ptrac- KAF6002099.1, Ctr-incA, CT_813*
4	SynBD3	pBD3	This study	*ΔNSII::CAT, Ptrac- PXF48205.1, Ctr-incA, CT_813*
5	SynBD4	pBD4	This study	*ΔNSII::CAT, Ptrac- XP_005707402.1, Ctr-incA, CT_813*
6	SynBD5	pBD5	This study	*ΔNSII::CAT, Ptrac- NP_178146.1, Ctr-incA, CT_813*
7	SynBD6	pBD6	This study	*ΔNSII::CAT, Ptrac- NC_003076.8, Ctr-incA, CT_813*
8	SynBD7	pBD7	This Study	*ΔNSII::CAT, Ptrac- CAX16542.1, Ctr-incA, CT_813*
9	SynBDsnare	pBD8	This study	*ΔNSII::CAT, Ptrac- Ctr-incA, CT_813*
10	SynBD8	pBD9	This study	*ΔNSII::CAT, Ptrac- TRINITY_DN12309, Ctr-incA, CT_813*

to export significantly lower levels of ATP when challenged with ADP compared to SynJEC3 (Fig. 3C, Supplementary Figs. 7-8). Next, we evaluated the red algae plastidic ADP/ATP carrier translocases (SynBD1-SynBD4). Unlike the plant plastidic ADP/ATP translocases, the red algae plastidic ADP/ATP translocase expressing strains SynBD2 (possess KAF6002099.1 gene) and SynBD3 (possess PXF48205.1 gene), were able to export significantly higher levels of ATP (~ 2.4-fold higher) compared to Syn7942 (wild-type) and ~ 1.5-fold higher ATP yield to SynJEC3 (possess CAE46506.1 gene from *Protochlamydia*[2]) (Fig. 3B). Given these surprising observations we next verified that both the red algal and land plant ADP/ATP carrier translocases were expressed. We added flag-tags to the algal PXF48205.1 and confirmed the expression in SynBD6 by western blot analysis (Supplementary Fig. 7). These data clearly demonstrated that the plastidic ADP/ATP carrier translocases from red algal strains had unexpected and distinct properties compared to the land plant plastidic ADP/ATP carrier translocase protein. Additionally, we also tested the putative translocase sequence (CAX16542.1) from the glaucophyte *C. paradoxa* but did not observe robust exchange activity (Supplementary Fig. 8A); however, it is important to note that these were partial sequences annotated based on metagenomic data. We then used high-quality genome assembly of a glaucophyte, *C. paradoxa*, to identify another putative ntt1 homolog, TRINITY_DN12309_ c0_g1_i1:235-2400. We made cyanobacterial mutants expressing this ntt1 homology and performed translocase assays with these strains (SynBD8). We observed higher levels of ATP export upon challenge with ADP as compared to the control wild-type strain, but lower levels as compared to SynJEC3 strain (Fig. 3E, Supplementary Fig. 8B). In contrast, significantly lower levels of ATP were detected in the supernatant of SynBD6 which expresses a thylakoid ADP/ATP carrier translocase (NC_003076.8) of the MCF subclass compared to the supernatants from Syn7942 and SynBD5 (Fig. 3C and Supplementary Fig. 9) when saturated with ADP. This was consistent with the previous report which suggests that the land plant plastidic ADP/ATP carrier translocases preferentially import ATP[37]. We added flag-tags to this protein as well and confirmed the expression in Syn7942 by western blot analysis (Supplementary Fig. 7). We also verified these key observations by expressing these translocases in *E. coli* and determining nucleotide exchange preferences (Supplementary Figs. 10–12).

To further investigate these observations, we next performed ATP uptake assays with Syn7942, SynBD2, SynJEC3, SynBD6 and SynBD8. Each of the mutant strains was incubated with defined levels of extracellular ATP (50 nM), the cells were centrifuged, and the cell medium was analyzed for ATP levels by using luciferase assays. No ATP was detected from the supernatant of SynBD6 whereas an abundant amount of residual ATP in the supernatant of Syn7942 (wild-type), SynJEC3, SynBD2 were detected (Fig. 3D). Lower levels of residual ATP were detected in SynBD8 strains as compared to SynJEC3 (Fig. 3E–F). Taken together, these data demonstrated differences in the preferences for ATP import versus export for the land plant plastidic MCF family belongs ADP/ATP transporters as compared to the ADP/ATP carrier transporters from red algal and glaucophytes.

Directed endosymbiosis to test cyanobacterial strains expressing ADP/ATP carrier translocases as yeast endosymbionts

In order to determine the relevance of our observations, i.e., different preferences for ATP import versus export to bioenergetics and endosymbiosis, we tested the key cyanobacterial mutant strains recombinantly expressing bioinformatically identified ADP/ATP carrier translocases as yeast endosymbionts (Fig. 4A)[23]. We anticipated that these experiments would allow us to test if the amounts of ATP released by endosymbiotic cyanobacterial mutants expressing recombinant translocases was enough to support ATP requirements of the host cells. Previously, we developed a directed endosymbiosis approach that allows us to generate bioenergetically necessary cyanobacterial endosymbionts within yeast cells under photosynthetic selection conditions. In this system, the yeast mutants *S. cerevisiae cox2-60* cells depend on ADP/ATP carrier translocase expressing cyanobacterial endosymbionts for ATP under defined photosynthetic selection conditions. We tested the key Syn7942 mutants (SynBD2, SynBD3, SynBD6 and SynJEC3) as yeast endosymbionts and evaluated the stability of the yeast/cyanobacteria chimeras. In order to generate the yeast/cyanobacteria chimeras, we used the fusion protocol that we had previously developed[23,30]. Briefly, we generated spheroplasts of *S. cerevisiae cox2-60* cells, fused them to engineered Syn7942 mutants (SynBD2, SynBD3, SynBD6, SynBD8, SynJEC3 and SynBDsnares) and selected the fusions by growing mixtures on partial selection conditions containing non-fermentable carbon source and low levels of fermentable carbon source (1% yeast extract, 2% peptone, 1 M sorbitol, 3 % glycerol, 0.1 % glucose, 1X BG-11; selection medium I). The fusions were propagated in 12 hours light-dark cycles at 30 °C. In each case, distinct colonies from *S. cerevisiae cox2*-60-cyanobacteria fusions were picked and re-plated for one round of regrowth: one round on selection medium II (1% yeast extract, 2% peptone, 1 M sorbitol, 3 % glycerol, 0.1 % glucose, 1X BG-11, 50 mg/mL carbenicillin; selection medium II) and five rounds on selection medium III (1% yeast extract, 2% peptone, 1 M sorbitol, 3 % glycerol, 50 mg/mL carbenicillin, 1X BG-11; selection medium III) till no growth of chimera cells (Fig. 4). Selection medium II and III contained carbenicillin to eliminate any extracellular cyanobacteria. The light microscopy view of control yeast *S. cerevisiae cox2-60* cells and fusion cells (SynJEC3, SynBD2 and SynBD3) are shown in (Supplementary Fig. 13). As expected, *S. cerevisiae cox2-60* cells failed to grow on selection medium III during subsequent rounds of regrowth when they were not fused to Syn7942. On the other hand, we observed relatively robust growth for *S. cerevisiae cox2-60*-SynBD2 and *S. cerevisiae cox2-60*-SynBD3 chimeras where the cyanobacteria expressed ADP/ATP carrier translocases from red algal plastids. In fact, the *S. cerevisiae cox2-60*-SynBD2 and *S. cerevisiae cox2-60*-SynBD3

https://doi.org/10.1038/s41467-024-54051-1

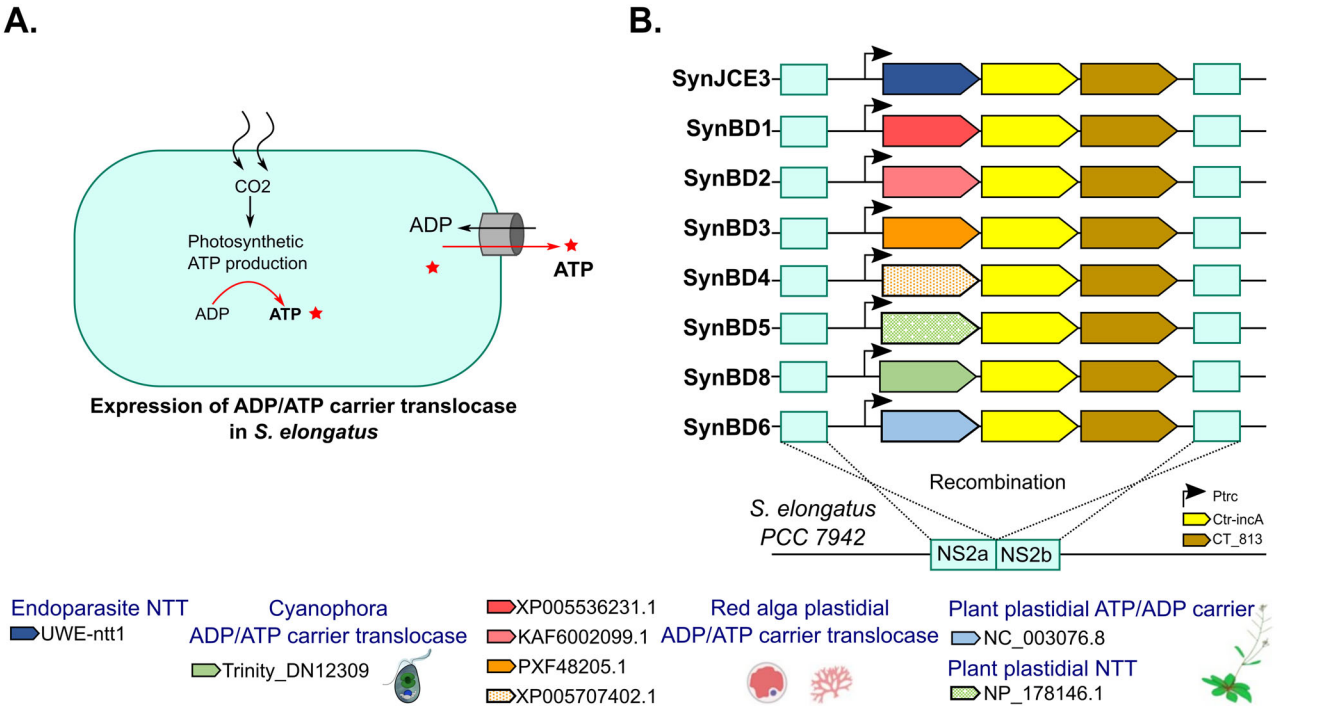

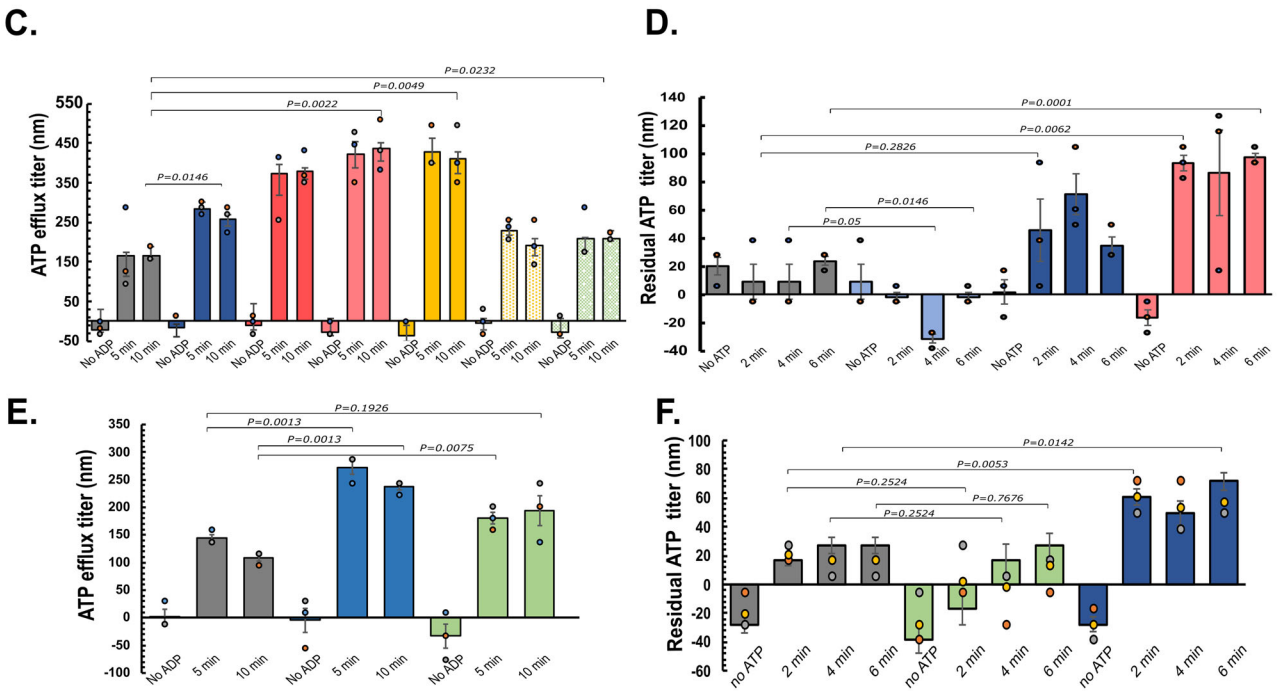

Fig. 3 | Cyanobacterial cell-based assays to study the properties of ADP/ATP carrier translocases. A Syn7942 mutants expressing bioinformatically identification of plastidic ADP/ATP carrier translocase proteins are used for ATP export/import assays. **B** Description of genetic recombination at the neutral site II (NS2) in the Syn7942 genome to afford engineered SynJEC3, SynBD1-8 strains (also see Table 1). The genomic DNA PCR analysis of mutant strains is shown in Supplementary Fig. 5. The color code neutral site II (NS2) in light gray box; endoparasite nucleotide transporter *CAE46506.1* gene in dark blue; red algal plastidic genes: *XP_005536231.1* gene in red, *KAF6002099.1* gene in light pink, *PXF48205.1* gene in orange, *XP005707402.1* gene in pattern red; plant plastidic nucleotide transporter *NP_178146.1* gene in pattern light green, *TRINITY_DN12309* gene in light green, plant plastidic mitochondrial family *NC_003076.8* gene in light blue; constitutive trc promoter in yellow bend arrow; genes encodind SNARE-like proteins *C.tr.-incA* in yellow and *CT_813* in brown. **C** ATP export was measured by luciferase assay. The Syn7942 (wild-type), engineered SynJEC3, SynBD1 to 5 cell counts were normalized. The cells were saturated with 80 μM ATP followed by wash and 80 μM ADP addition. Extracellular ATP was measured before ADP addition and after ADP addition (5 and 10 min). **D** Residual ATP titer was measured by luciferase assay. The Syn7942 (wild-type), SynJEC3, SynBD2 and SynBD6 cell counts were normalized. The cells were incubated with 50 nM ATP and the residual ATP was measured at various time points. **E** ATP export for measured for Syn7942 (wild-type), SynJEC3, SynBD8 as described previously. **F** Residual ATP titer was measured for Syn7942 (wild-type), SynJEC3, SynBD8 as described previously. The color code bar for Syn7942 in gray bar, SynJEC3 blue bar, SynBD1 in red, SynBD2 light pink, SynBD3 light brown, SynBD4 pattern brown, SynBD5 pattern green, SynBD6 in light blue bar and SynBD8 in light green bar. All assays were performed in triplicate ($n = 3$ technical replicates; data are presented as mean values +/− SEM). *P*-values were calculated by two-tailed *t*-test comparing the two means. Source data are provided as a Source Data file.

https://doi.org/10.1038/s41467-024-54051-1

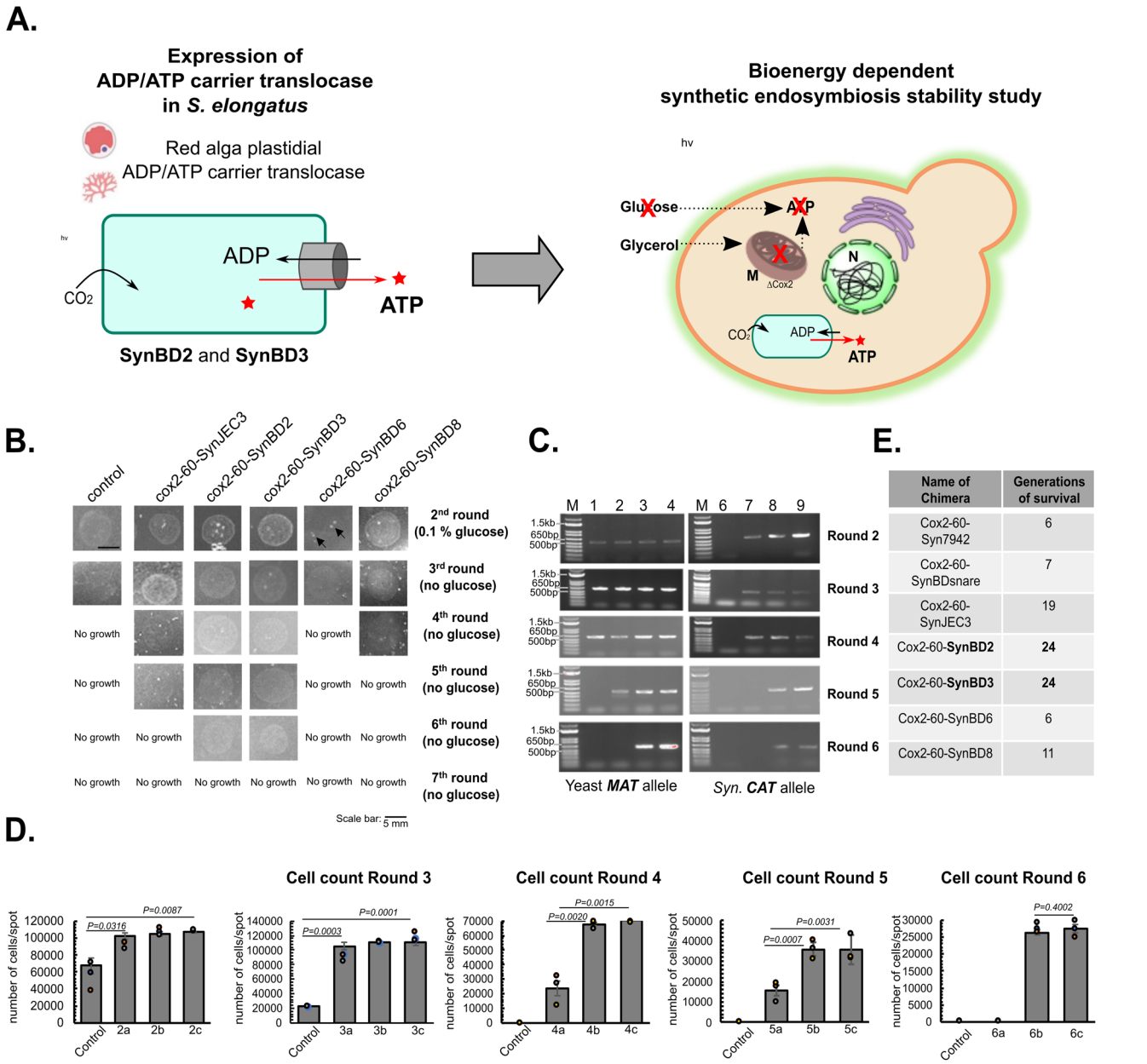

Fig. 4 | Directed endosymbiosis. A Schematic representation of ATP dependent directed endosymbiosis. **B** Spot growth of yeast/cyanobacteria chimeras for multiple rounds on selection conditions. **C** Genomic DNA PCR to detect yeast *MAT* allele and *CAT* gene for engineered cyanobacterial mutants. M is for DNA ladder, MAT allele amplification from round 2 to 6 were shown at lane 1: control host yeast, lane 2 to 4: *S. cerevisiae cox 2-60*-SynJEC3, BD2 and BD3. *CAT* gene amplification shown at lane 6: control host yeast (No *CAT* gene were amplified for host control yeast cells); *S. cerevisiae cox 2-60*-SynJEC3 (no *CAT* gene amplification from round 5 onward represents absence of synJEC3), *S. cerevisiae cox 2-60*-SynBD2 and BD3 can be seen till round 6. **D** Cell count analysis from round 2 to round 6 cell propagation. The bar graph was presented as Control: yeast cells; 2-6a represents *S. cerevisiae cox 2-60*-SynJEC3 cell counts from second round to round five. 2-6b *S. cerevisiae cox 2-60*-SynBD2 cell counts from second round to round six; and 2-6c represents *S. cerevisiae cox 2-60*-SynBD3 cell counts from second round to round six. Data represents the mean of three independent experiments. Error bars are displayed. **E** An approximate viability of yeast/cyanobacteria chimeras was calculated based on chimera cells count and doubling. All Cell counts were performed in triplicate ($n = 3$ biological replicates; data are presented as mean values +/− SEM). ($n = 3$ biological replicates; data are presented as mean values +/− SEM). Error bars are displayed. Two-sided *t*-tests were used to compare means without adjustments. Source data are provided as a Source Data file.

chimeras were stable for up to six rounds of regrowth (at least 24 doublings) compared to *S. cerevisiae cox2-60*-SynJEC3 chimeras that were stable for four rounds of regrowth (~19 doublings) under identical photosynthetic selection conditions (Fig. 4). On the other hand, the *S. cerevisiae cox2-60*-SynBD6 chimeras, where the cyanobacteria expressed ADP/ATP carrier translocases from land plant, was viable only for around 6 rounds of doubling (Fig. 4, Supplementary Fig. 14). Furthermore, the *S. cerevisiae cox2-60*-SynBDsnares chimeras, where the cyanobacterial mutants lacked recombinant ntt1 but possessed SNAREs, were viable for around 7 doublings (Supplementary Fig. 15). These observations clearly highlighted the importance of biochemical properties of ntt1 homologs to support ATP driven endosymbiosis. Fusions with *S. cerevisiae cox2-60* and SynBD8, where the cyanobacteria expressed ADP/ATP carrier translocases from glaucophyte, resulted in the generation of *S. cerevisiae cox2-60*-SynBD8 chimeras. We observed higher number of doublings for these chimeras as compared to the control chimeras with SynBDsnares lacking recombinant ntt1 expression (Fig. 4B–D and Supplementary Figs. 15–16).

These chimeras were relatively less robust (based on doubling numbers) as compared to *S. cerevisiae cox2-60*-SynBD2 and *S. cerevisiae cox2-60*-SynBD3 chimeras (Fig. 4B–D, and Supplementary Fig. 16). These experiments correlate the ATP secretion potential of cyanobacterial endosymbionts to the viability of the ATP driven endosymbiosis of these yeast/cyanobacteria chimera.

To characterize the presence of cyanobacterial endosymbionts within yeast cells, in each of the cases we isolated total genomic DNA from fused yeast cells propagated for multiple generations under selection growth conditions and performed PCR analysis to determine the presence of both yeast and cyanobacterial genomes. We detected the presence of both the yeast *MATa* gene and mutant Syn7942 chloramphenicol acetyltransferase (*CAT*) gene in the colonies by PCR (Fig. 4B and Supplementary Figs. 14–16), suggesting the presence of both yeast and cyanobacterial genomes. The number of generations for which we observed the viability of the yeast/cyanobacteria chimeras is listed in Fig. 4E. We also verified the dependence of these yeast/cyanobacteria chimeras on photosynthesis by demonstrating the necessity of light for robust propagation and the lack of growth on adding (3-(3,4-dichlorophenyl)-1,1-dimethylurea, DCMU), an inhibitor of photosynthesis (Fig. 5A–D).

These experiments suggested that the cyanobacteria that express ADP/ATP carrier translocases from the red algae plastids and glaucophyte plastids were able to support the bioenergetic requirements of the yeast/cyanobacteria chimeras more robustly under photosynthetic selection as compared to the cyanobacteria expressing ADP/ATP carrier translocases from the land plant plastids.

Imaging key yeast/cyanobacteria mutant chimeras

In order to evaluate the endosymbiotic chimeras, the cells were propagated under selection conditions for multiple passages and then imaged by using both total internal reflection fluorescence (TIRF) and fluorescence confocal microscopy approaches to detect the presence of cyanobacterial endosymbionts within the yeast cells (Fig. 6 and Supplementary Fig. 17)[23]. The fluorescence of cyanobacterial chlorophyll and phycobilin allowed us to use total internal reflection fluorescence (TIRF) laser microscopy at 650 nanometer (nm) emission to detect cyanobacteria. The merged images of bright field and laser emission (650 nm) demonstrated the presence of cyanobacterial endosymbionts within the yeast cells for each of the yeast cyanobacteria chimeras, *S. cerevisiae cox2-60*-SynJEC3, *S. cerevisiae cox2-60*-SynBD2, *S. cerevisiae cox2-60*-SynBD3 and *S. cerevisiae cox2-60*-SynBD8 (Fig. 6A–B). The yeast/cyanobacteria chimeras were imaged for multiple generations of growth under selection conditions, and in each case, we detected the presence of cyanobacterial signals within the yeast cells (Supplementary Fig. 17A) until we observed growth under selection conditions. We also performed fluorescence confocal microscopy to confirm these observations. For this imaging, we fixed the chimeras and stained the yeast membranes with FITC-labeled concanavalin A and performed imaging using a commercial Leica SP8 fluorescence confocal microscope (Fig. 6 and Supplementary Fig. 17A). The confocal microscope was set to two different wavelengths, excitation using 488 nm laser and emission at 510-520 nm for Conn A-FITC and excitation at 561 nm with emission at 561 nm for cyanobacteria[23]. We tracked the cyanobacterial signals for multiple rounds of regrowth and again we detected cyanobacterial signals within the yeast cells (Supplementary Fig. 17B) until we observed growth under selection conditions (Fig. 6B). We also detected the presence of cyanobacteria-like structures by using transmission electron microscopy (TEM), (Supplementary Fig. 18). Consistent with our phenotypic growth data, these sets of experiments clearly demonstrated the robustness of the cyanobacterial endosymbionts expressing red algal plastidic ADP/ATP carrier translocase in our directed endosymbiosis platform.

Discussion

Organelles like mitochondria and chloroplasts are one of the endpoints of endosymbiosis. It is generally accepted that chloroplasts evolved from cyanobacterial endosymbionts that were established within eukaryotic cells. The key metabolic drivers that led to the establishment of cyanobacterial endosymbionts are still unclear[6]. It is suggested that that bioenergetic factors (e.g., dependence of host cells on endosymbionts for ATP synthesis) may have been crucial for endosymbiosis and organelle evolution[6,7]. In case of mitochondria, the ATP synthesized by oxidative phosphorylation of ADP whereas in case of chloroplast the ATP is synthesized by photophosphorylation of ADP. Since the key role of mitochondria is fulfilling the ATP requirements of the cell, the mitochondria express ADP/ATP carrier translocases to preferentially exchange synthesized ATP with cytosolic ADP. While the present-day chloroplasts also possess ADP/ATP carrier translocases, they are generally suggested to have varied preferences for ATP import versus export as compared to the mitochondrial ADP/ATP carrier translocases. In case of the plant chloroplasts, ADP/ATP carrier translocase are suggested to be expressed and functional during different stages as the plant cell cycles between photosynthesis and dark cycle[28,39]. The ADP/ATP carrier translocase from *Arabidopsis thaliana* preferentially imports ATP and are suggested to be crucial to sustain the metabolic functions of the plant plastids[37]. Evolutionary studies suggest that the endosymbiotic cyanobacteria, a precursor of chloroplast, may have acquired ADP/ATP carrier translocases through horizontal gene transfer from parasitic strains belonging to *Chlamydiales*[8,13].

Based on these observations, we hypothesized that studying the preferences of ADP/ATP carrier translocases from key lineages of photosynthetic eukaryotes, i.e., red algae, glaucophytes and land plants, could provide insights into the role of bioenergetics in the context of chloroplast evolution. Using bioinformatics analysis, we first identified a few putative plastidic ADP/ATP carrier translocases from these lineages. Next, we determined the preferences of these plastidic ADP/ATP carrier translocases for ATP export versus import. Since properties of translocases are indicative of organelle function[8,9,11,12], we believe that understanding these preferences could highlight the differences in organelle functions in photosynthetic eukaryotes. Using cyanobacterial cell-based translocase assays and ATP uptake assays we observed that representative plastidic ntt1 homologs from different lineages of photosynthetic eukaryotes had differing preferences for ATP export versus ATP import. Particularly, we observed that the cyanobacterial cells expressing plastidic ADP/ATP carrier translocases from red algal and glaucophytes exported ATP when challenged with extracellular ADP. On the other hand, the cyanobacterial cells expressing ADP/ATP carrier translocases from land plant plastids secreted very low levels of ATP when challenged with extracellular ADP and also imported higher levels of ATP. To determine the relevance of our observations to endosymbiosis and bioenergetics, we tested cyanobacterial mutant strains recombinantly expressing bioinformatically identified ADP/ATP carrier translocases as yeast endosymbionts. We observed that the cyanobacterial mutants expressing ADP/ATP carrier proteins that were competent to export ATP were able to establish ATP-dependent endosymbiosis with yeast mutants whereas the cyanobacterial mutants expressing ADP/ATP carrier proteins that imported ATP were unable to establish ATP-dependent endosymbiosis with yeast mutants. These artificially directed endosymbiosis approaches demonstrated the relevance of different preferences for ATP import vs export on endosymbiont function and stability of bioenergetically driven endosymbiosis.

Our observations could potentially have implications on the evolution of photosynthetic eukaryotes. As mentioned earlier, red algal plastids have compacted and gene-rich architectures that most closely resemble the plastid ancestors, lack of unique unknown ORFs, highly conserved gene order, and slower rate of plastid-to-nucleus

https://doi.org/10.1038/s41467-024-54051-1

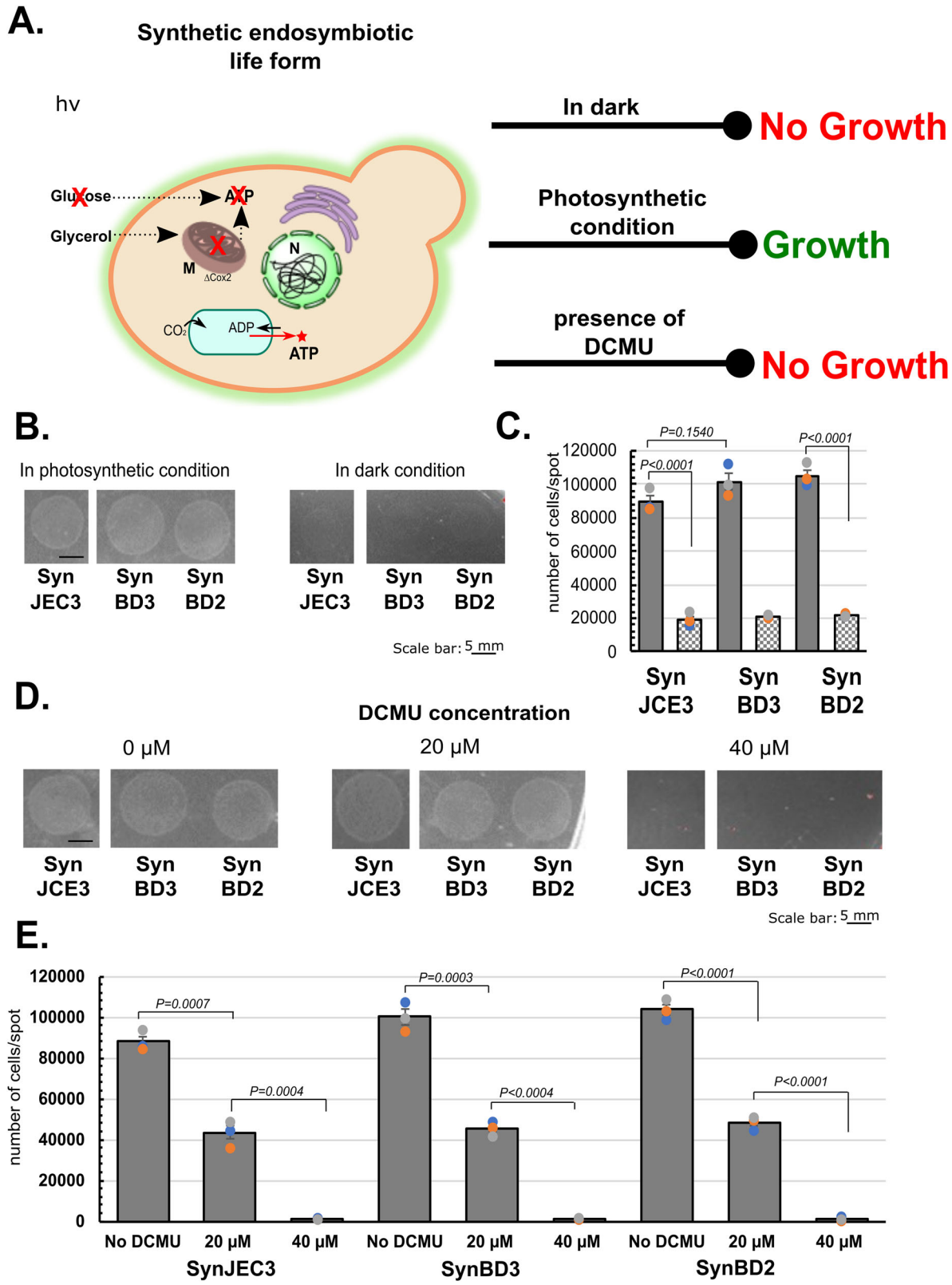

gene transfer amongst others[17,18]. Additionally, glaucophyte plastids have retained several molecular trait from their cyanobacterial ancestors (e.g., peptidoglycan wall between the organelle membranes[19], similar composition of their photosynthetic apparatuses[20]) making them an attractive target to investigate the evolution of primary plastids[21,22]. The plastidic ntt1 homologs from red algae and glaucophytes that we identified, showed properties that were distinct from the land plant plastidic ntt1 homologs. Based on these studies, one hypothetical scenario would be that the initial interaction between chloroplast and host cell was based on ATP production by the cyanobacterial endosymbiont. Over the course of evolution, the cyanobacterial endosymbionts may have transformed from ATP and assimilated carbon-providing endosymbionts into land plant chloroplasts that primarily provide assimilated carbon sources

Fig. 5 | Dependence of yeast/cyanobacteria chimeras on photosynthesis. **A** Schematic representation to study the growth dependence on yeast/cyanobacteria chimeras on photosynthesis. **B** Spot growth of yeast/cyanobacteria chimeras for multiple rounds under photosynthetic selection conditions or in absence of light (dark conditions). The experiment was repeated three times independently with similar results. **C** The bar diagram presenting the chimeras growth, and their cell count after 72 hours. Error bars are displayed. **D** Growth of round 3 Yeast *S. cerevisiae cox 2-60*-SynJEC3, *S. cerevisiae cox 2-60*-SynBD2, *S. cerevisiae cox 2-60*-SynBD3 chimeras on Selection Medium III in presence of DCMU, final concentration 0 μM or 20 μM or 40 μM. 10,000 cells were propagated in each spot followed by incubation for 72 hours under photosynthetic day/night cycle. The experiment was repeated three times independently with similar results. **E** The bar diagram presenting the chimeras growth, and their cell count after 72 hours of incubation in presence of DCMU with photosynthetic day/night. All Cell counts were performed in triplicate ($n = 3$ biological replicates; data are presented as mean values +/− SEM). Error bars are displayed. Two-sided *t*-tests were used to compare means without adjustments. Source data are provided as a Source Data file.

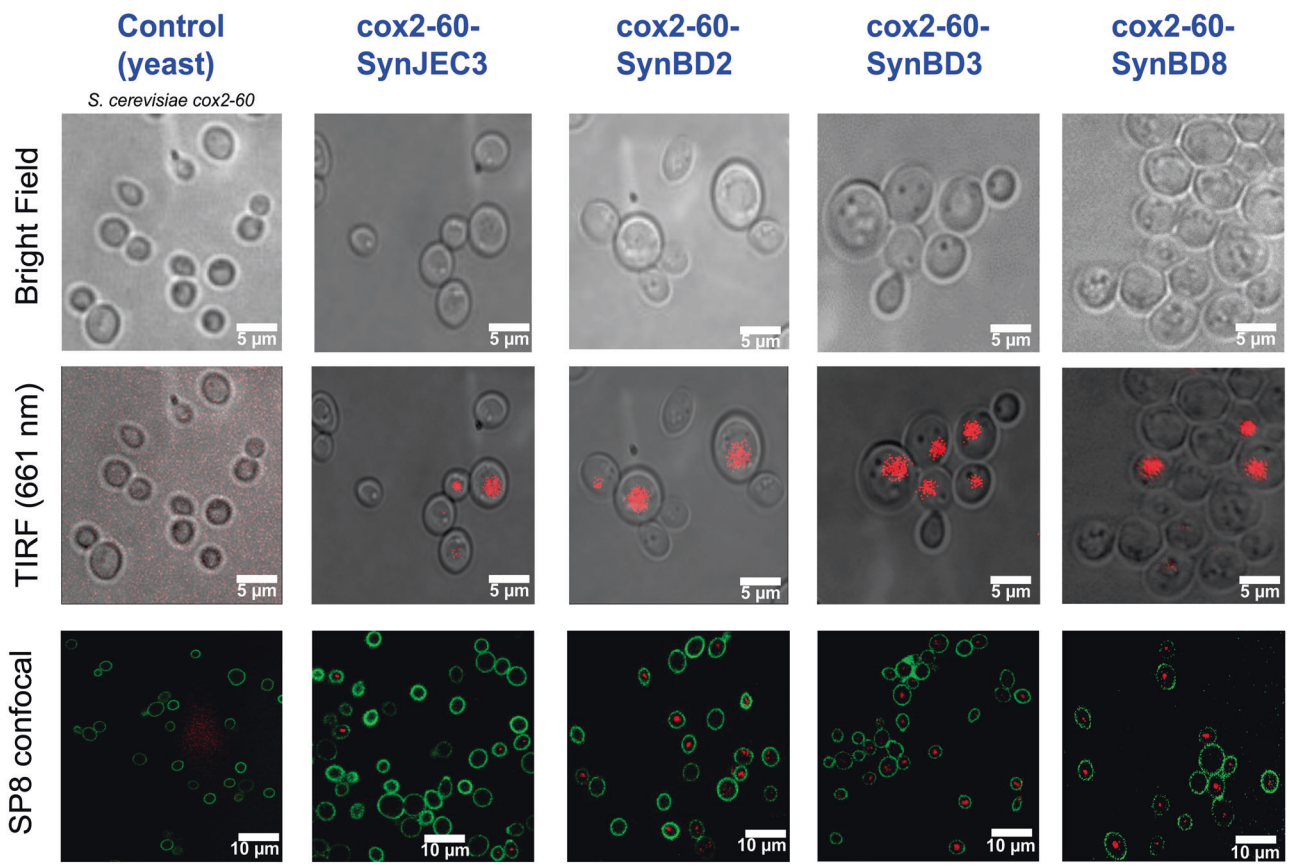

Fig. 6 | Imaging studies of the yeast/cyanobacteria chimeras. Bright field microscopic image corresponding to pTERF image showing control *S. cerevisiae cox 2-60*, and chimeras *S. cerevisiae cox2-60*-SynJEC3, *S. cerevisiae cox2-60*-SynBD2, *S. cerevisiae cox2-60*-SynBD3 and *S. cerevisiae cox2-60*-SynBD8. Marged image of bright field chimeric cells (at gray) and pTIRF (X100) microscopic images can be predicted using 561 nm laser for visualization of endosymbiont autofluorescence chlorophyl (in red Em.=653/95 nm) from photosynthetically enabled engineered Syn. No such signal was detected from control yeast cells. SP8 Fluorescent confocal microscopic (x63) image of control *S. cerevisiae cox 2–60*, and endosymbiontic chimera. Marged images: host cell was stained using Conn A-FITC (emission at 510–520 nm wavelength, in green) and cyanobacterial autofluorescence can detected at 616-650 nm wavelength range. The experiment was repeated three times independently with similar results.

for other bioenergetically important processes like glycolysis. Further, as mitochondria continued to evolve into specialized organelles that were efficient in ATP synthesis, the chloroplasts in land green plants which grow in relatively abundant oxygen conditions, might have started to evolve into organelles whose primary function was to provide assimilated carbon sources (e.g., sugars) to the host cell rather than photosynthetically generated ATP. Another hypothetical scenario would be that the ATP secretion from these red algal and glaucophyte plastids was an adaptation feature in response to their ecology (e.g., underwater growth in limiting oxygen concentrations). These intriguing hypotheses could be further tested directly in relevant organisms. Further, these approaches can be used to study host/endosymbiont adaptation factors in ATP driven endosymbiosis, the fitness cost of endosymbiont, and host mediated control over endosymbiont numbers. Additionally, the synthetic cyanobacterial endosymbionts we generated in this study may also have implications for various sustainable synthetic biology applications (e.g., photosynthetic metabolic engineering[25], carbon dioxide sequestration).

Methods

Bacterial strains, compounds, and reagents

Synechococcus elongatus strains were derived from *Synechococcus elongatus* PCC 7942 (Syn7942). This strain was obtained from Prof. Susan Golden's lab (University of California San Diego, UCSD). We used *S. cerevisiae* ρ+(MATa leu2-3,112 lys2 ura3-52 his3ΔHindIII arg8-Δ::URA3 [cox2-60])[30] as a host for *S. elongatus* endosymbionts.

Sequence similarity networks analysis of CAE46506 homologs

Sequence similarity networks (SSN) analysis was based on the PSI-BLAST (Position-Specific Iterated BLAST) search using nucleotide

transporter (NTT) protein from *Candidatus Protochlamydia amoebophila* UWE25 (NCBI Sequence ID CAE46506.1) as a query sequence. By using the NCBI database, non-redundant protein sequences (nr) we curated 500 sequences as prelimany data. In addition, organism specific PSI-BLAST was performed, for red algae (taxid:2763) and higher plants (taxid:3193). There are a total of 500 sequences of non-redundant protein sequences (nr) which have identity coverage of 48.44 to 100 % with query coverage of 92 to 100%. Similarly top 500 sequences were selected from higher plants (taxid:3193) which have identity coverage of 48.44 to 100 % and query coverage of 91 to 97%. Finally, red algal protein hits were selected with identity coverage of 53.22 to 57.03% and query coverage of 73 to 96%. The EFI- Enzyme Similarity Tool (EFI-EST, https://efi.igb.illinois.edu/efi-est/) was used to generate sequence similarity networks (SSNs). A data set of 1010 sequences was used to build the SSN. An alignment score of 120 was used for generating the networks described in this study.

Identification of *Cyanophora paradoxa* ADP/ATP translocase and phylogenetic analysis

Identification of complete glaucophyte *Cyanophora paradoxa* putative ADP/ATP translocase performed after BLASTp search to whole genome data base (http://cyanophora.rutgers.edu/cyanophora_v2018/) using CAX16542.1 (partial sequence) as query sequence. The identified complete *Cyanophora paradoxa* putative ADP/ATP translocase TRINITY_DN12309_c0_g1_i1:235-2400 (http://cyanophora.rutgers.edu/cyanophora_v2018/, TransDecoder) was included for further multiple sequence alignment and phylogenetic analysis. In order to get a better view of NTT and ADP/ATP translocase diversity, a small dataset contains total 104 sequences were selected from endoparasite, archaea, protozoa, metazoan, dinoflagellates, euglena, chlorella, red algae, heterokonta, diatoms, green algae, moss, glaucophytes, higher plants (Fig. 2C). All retrieved FASTA sequences were aligned by Clustal Omega online multiple sequence alignment tool (https://www.ebi.ac.uk/Tools/msa/clustalo/). A phylogenetic tree was constructed using MEGA11 software, employing the Maximum Likelihood method and the JTT matrix-based model, with 500 rapid bootstrap replicates. The tree with the highest log likelihood (-9419.02) is shown. A discrete Gamma distribution was used to model evolutionary rate differences among sites (5 categories (+ *G*, parameter=0.9047)). The rate variation model allowed for some sites to be evolutionarily invariable ([+*I*], 11.68% sites). Finally, the phylogenetic tree (Fig. 2C and Supplementary Fig. 1) was visualized by iTOL[40].

Construction of plasmids

Primers and gBlock gene fragments were purchased from Integrated DNA Technologies (IDT). Primers are listed in Supplementary Data 3. DNA fragments were amplified by Polymerase Chain Rreaction, PCR (Q5 Hot Start High-Fidelity 2X Master mix, NEB catalog # M0494S), and assembled into vectors by Gibson assembly. Gene fragments of ADP/ATP carrier genes are listed in Supplementary Table 1 and Supplementary Data 1. The genes were codon-optimized for *S. elongatus* expression using IDT codon optimization browser tool (https://www.idtdna.com/CodonOpt). Cyanovectors were obtained from Prof. Susan Golden's lab (UCSD). Cloning vectors were transformed into One Shot® ccdB Survival™ 2 T1R Chemically Competent Cells (Invitrogen A10460) according to manufacturer's specifications.

The plasmids pBD1 – pBD6 are derived from the pML17 (Supplementary Data 2). Vector maps are included in Supplementary Fig. 4, and detailed vector map links are provided in Supplementary Table 2.

pML+ XP_005536231.1: pML17 was linearized by PCR using the oligonucleotides pML17_F/ R. A gBlock of the *Cyanidioschyzon merolae* strain 10D; *XP_005536231.1* gene codon optimized for *S. elongatus* was amplified by PCR using the oligonucleotides BD2F/R. The amplified DNA fragment was inserted into linearized pML17 by Gibson assembly to afford pBD1.

pML+ KAF6002099.1: A codon optimized gBlock of the *Cyanidiococcus yangmingshanensis KAF6002099.1* gene was amplified by PCR using the oligonucleotides BD3F/R and inserted into linearized pML17 by Gibson assembly to afford pBD2.

pML+ PXF48205.1: A codon optimized gBlock of the *Gracilariopsis chorda PXF48205.1* gene codon-optimized for *S. elongatus* was amplified by PCR using the oligonucleotides BD4F/R and inserted into linearized pML17 by Gibson assembly to afford pBD3.

pML+ XP_005707402.1: A codon optimized gBlock of the *Galdieria sulphuraria XP_005707402.1* gene was amplified by PCR using the oligonucleotides BD5F/R and inserted into linearized pML17 by Gibson assembly to afford pBD4.

pML+ NP_178146.1: A codon optimized gBlock of the *Arabidopsis thaliana NP_178146.1* gene was amplified by PCR using the oligonucleotides BD6F/R and inserted into linearized pML17 by Gibson assembly to afford pBD5.

pML+ NC_003076.8 (locus_tag=AT5G01500): A codon optimized gBlock of the *Arabidopsis thaliana NC_003076.8* gene was amplified by PCR using the oligonucleotides BD7F/R and inserted into linearized pML17 by Gibson assembly to afford pBD6.

pML+CAX16542.1: A codon optimized gBlock of the *Cyanophora paradoxa CAX16542.1*gene was amplified by PCR using the oligonucleotides BD11F/R and inserted into linearized pML17 by Gibson assembly to afford pBD7.

pML+PXF48205.1-Flag: A same codon optimized gBlock of the *Gracilariopsis chorda PXF48205.1-flag* gene codon-optimized for *S. elongatus* was amplified by PCR using the oligonucleotides BD8F/R. The pML17 back bone was PCR isolated using BD9F/R and inserted into linearized pML17 by Gibson assembly to afford pBD3-flag.

pML+NC_003076.8-Flag: A codon optimized gBlock of the *Arabidopsis thaliana NC_003076.8-flag* gene was amplified by PCR using the oligonucleotides BD10F/R and inserted into linearized pML17 by Gibson assembly to afford pBD6-flag.

pML_SNARE: The SNARE genes encode Ctr-incA, and CT_813 genes were PCR isolated using oligonucleotides BD13F/1R. The linear vector backbone was PCR amplified using oligonucleotides BD15F/16 R. Performed Gibson assembly to afford pBD8.

pML+TRINITY_DN12309: A codon optimized gBlock of the *Cyanophora paradoxa TRINITY_DN12309* gene was amplified by PCR using the oligonucleotides BD7F/R and inserted into linearized pML17 by Gibson assembly to afford pBD9.

Engineering of cyanobacteria strains

Log-phase Syn7942 cultures (15 mL) were centrifuged for 10 min at 3000 × *g* and 24 °C. The pellet was washed with 10 mL NaCl (10 mM) and resuspended in 0.3 mL BG-11 at room temperature. To this suspension was added the plasmid (1.5 µL), and the mixture was added to a 1.5 mL microcentrifuge tube and shaken in the dark (12–16 h at 70 rpm). Transformed cells were spread on BG-11 agar plates supplemented with appropriate antibiotic(s) and incubated at 37 °C under 30-50 µmol photons·$s^{-1}m^{-2}$ for ≤10 days. PCR analysis of recombinant loci was used to evaluate genomic recombination.

SynJEC3 was generated by transformation of wild-type Syn7942 with pML17 to give a recombinant mutant which ectopically expresses Ctr-incA, CT813 and an ADP/ATP translocase from the NSII locus.

SynBD1 was generated by transformation of wild-type Syn7942 with pBD1 to give a recombinant mutant which ectopically expresses Ctr-incA, CT813 and *Cyanidioschyzon merolae* strain 10D *XP_005536231.1* a putative chloroplast ADP/ATP translocase from the NSII locus.

SynBD2 was generated by transformation of wild-type Syn7942 with pBD2 to give a recombinant mutant which ectopically expresses Ctr-incA, CT813 and *Cyanidiococcus yangmingshanensis KAF6002099.1* a putative ADP/ATP carrier from the NSII locus.

SynBD3 was generated by transformation of wild-type Syn7942 with pBD3 to give a recombinant mutant which ectopically expresses Ctr-incA, CT813 and *Gracilariopsis chorda PXF48205.1* a putative chloroplast ADP/ATP translocase from the NSII locus.

SynBD4 was generated by transformation of wild-type Syn7942 with pBD4 to give a recombinant mutant which ectopically expresses Ctr-incA, CT813 and *Galdieria sulphuraria XP_005707402.1* a putative ADP/ATP translocase from the NSII locus.

SynBD5 was generated by transformation of wild-type Syn7942 with pBD5 to give a recombinant mutant which ectopically expresses Ctr-incA, CT813 and *Arabidopsis thaliana NP_178146.1* a putative ADP/ATP translocase from the NSII locus.

SynBD6 was generated by transformation of wild-type Syn7942 with pBD6 to give a recombinant mutant which ectopically expresses Ctr-incA, CT813 and *Arabidopsis thaliana NC_003076.8* a putative thylakoid an ADP, ATP carrier protein from the NSII locus.

SynBD3-Flag was generated by transformation of wild-type Syn7942 with pBD3-flag to give a recombinant mutant which ectopically expresses Ctr-incA, CT813 and *Gracilariopsis chorda PXF48205.1-Flag* a putative plastidic ADP/ATP translocase from the NSII locus.

SynBD6-Flag was generated by transformation of wild-type Syn7942 with pBD6-flag to give a recombinant mutant which ectopically expresses Ctr-incA, CT813 and *Arabidopsis thaliana NC_003076.8* a putative thylakoid an ADP, ATP carrier protein from the NSII locus.

SynBDsnare strain was generated by transformation of wild-type Syn7942 with pBD8 to give a recombinant mutant which ectopically expresses Ctr-incA, CT813 proteins from the NSII locus.

SynBD7 strain was generated by transformation of wild-type Syn7942 with pBD7 to give a recombinant mutant which ectopically expresses Ctr-incA, CT813 proteins from the NSII locus.

SynBD8 strain was generated by transformation of wild-type Syn7942 with pBD9 to give a recombinant mutant which ectopically expresses Ctr-incA, CT813 proteins from the NSII locus.

Luciferase assay to measure ATP release by engineered cyanobacteria

Trace levels of contaminating ATP was removed from ADP solution (Sigma A2754) through treatment with hexokinase: ADP (80 mM, pH 7.5) was incubated with D-glucose (200 mM), $MgCl_2$ (2 mM) and hexokinase (Sigma H4502-500UN) (0.04 U/μL) at room temperature for 2 h. The mixture was filtered through an Amicon Ultra 0.5 column (14,000 × *g*, 15 min) and the flowthrough was stored at -20 °C. Syn7942 (wild-type), SynBD1 to SynBD5 cells were grown for 3 d to reach densities of OD_{750} of 0.6. For each assay, cells were harvested by centrifugation (3000 × *g*, 5 min, room temperature), and washed with 20 mM Tris-HCl buffer (pH 8.0). The cells were normalized to a density (OD_{750}) of 1.5. The normalized cells were then incubated with ATP solution (Sigma G8877) (10 mM, pH 7.5) for 15 min at 37 °C and washed three times with 20 mM Tris-HCl to eliminate extracellular ATP. ADP (80 μM final concentration) was added, and the cells were incubated at 37 °C. The suspensions were centrifuged (10,000 × *g*, 5 min) and the supernatant ATP concentration was determined by using luciferase assay (ATP determination kit, Life Technologies - #A22066). ATP standards (provided with the kit) were used to obtain calibration curves.

Luciferase assay to measure ATP uptake

Syn7942 (wild-type), SynBD2, SynBD3 to SynBD6 cells were grown for 3 days to reach densities of OD_{750} of 0.6. For each assay, cells were harvested by centrifugation (3000 × *g*, 5 min, room temperature), and the pellet was washed once with 20 mM Tris-HCl buffer (pH 8.0). The cells were normalized to OD_{750} of 1.5. The cells were kept in dark for overnight prior to incubation with ATP. The normalized cells were then incubated with ATP solution (Sigma G8877) (50 nM, pH 7.5) at 37 °C for 2, 4, 6 minutes. The mixtures were then centrifuged (10,000 × *g*, 5 min) and the supernatant ATP concentration was determined by using luciferase assay (ATP determination kit, Life Technologies - #A22066). ATP standards (provided with the kit) were used to obtain calibration curves.

Western blot analysis for ADP/ATP carrier translocase protein expression in Syn7942 study

Syn7942 control strain and SynBD3-Flag strain were grown in appropriate culture medium describe above at 37 °C, 3000 lux till OD730 ~ 1.2. The cells were resuspended in lysis buffer (50 mM Tris-HCl, pH 8, 5 % SDS, 1 mM β-mercaptoethanol) and lysed by heating them at 90 °C for 10 min. The cell lysate was mixed with 1x Laemmli sample buffer (BIO-RAD, USA). SDS-PAGE was performed after loading 200 μg protein in 12 % acrylamide protein gels. Gel was then stained for total protein using SYPRO Ruby (Invitrogen), according to the manufacturer's instructions, or used for western blot. For western blot analysis, gels were transferred to an Millipore Immobilon-P 0.45 μm polyvinyl fluoride (PVDF) membrane in NuPAGE transfer buffer (Invitrogen) for 180 min at 60 V in a XCell blot module (Invitrogen) at cold room and the membrane was then incubated in blocking solution (TBS-T; 20 mM Tris-Cl, 150 mM NaCl, 0.02% (v/v) Tween-20, pH 7.6 supplemented with 5% (w/v) non-fat dry milk) for 1 h. All incubation steps were carried under shaking conditions on a rocking table. Blocking agent was discarded and the membrane was incubated with primary antibody−Anti-FLAG Rabbit mAb (Cell Signaling Technology, Catalog # 14793S) used 1: 1000 dilution and 1:12000 secondary antibody−Anti-Rabbit IgG (Sigma, Catalog # A0545). Membranes were washed for 3 × 5 min in TBS-T then incubated for 5 min in ECL substrate consisting of 0.5 mL each of SuperSignal West Dura reagent A and B (Thermo Scientific) and imaged using an iBright 750 (Invitrogen) imaging system.

Fusion of engineered cyanobacteria to *S. cerevisiae cox2-60* cells

The standard cell fusion protocol was followed.[23,25,30,38] Briefly, SynJEC3, SynBD2, SynBD3 and SynBD6 engineered mutants were grown under constant light (30-50 μmol photons·$s^{-1}m^{-2}$), with shaking, for 4 days. The cells (30 mL) were then harvested (3000 × *g*, 10 min, 24 °C), washed twice with BG-11 and resuspended in BG-11 (500 μL). *S. cerevisiae* cox2-60 was grown aerobically in YPD medium (500 mL) in a 1-liter conical flask for 20 h with shaking at 200 rpm at 30 °C. The yeast cells were harvested (2500 × *g*, 10 min, 30 °C), washed twice with sterile water, twice with SCEM (1 M sorbitol, 13 mM β-mercaptoethanol) and resuspended in filtered SCEM solution (10 mL) containing Zymolyase 100 T (15 mg total). The suspension was incubated for 1 h at 37 °C resulting in complete spheroplasting of the culture. The suspension was centrifuged for 10 min at 1500 × *g* at rt. The pellet was washed twice with SCEM solution at room temperature and resuspended in 1 mL SCEM. The spheroplast suspension (5 × 750 μL) was mixed with TSC buffer (10 mM Tris-HCl, 10 mM $CaCl_2$, 1 M sorbitol, pH 8) (750 μL) and incubated for 10 min at 30 °C in a microcentrifuge tube. The mixture was centrifuged (1500 × *g*, 10 min) and the supernatant was carefully discarded. The spheroplasts were resuspended in room temperature TSC buffer (5 ×120 μL) and sorbitol (4 M, 60 μL). The prepared *S. elongatus* cell suspensions SynJEC3, SynBD2, SynBD3 and SynBD6 (120 μL) were added quickly to the spheroplast suspensions, mixed by tube inversion and incubated statically for 30 min at 30 °C. This mixture was then decanted into a round-bottom polypropylene tube containing PEG buffer (20% PEG 8000, 10 mM Tris-HCl, 2.5 mM $MgCl_2$, 10 mM $CaCl_2$, pH 8) (2 mL) and incubated statically at 30 °C for 45 min. The cells were centrifuged (1500 × *g*, 10 min, 24 °C), the supernatant was discarded and 1 mL of YPDS (YPD with 1 M sorbitol added) was added on top of the plating. The cells were incubated under light without shaking for 2 h at 30 °C under 30 rpm. The pellet was then dislodged by flicking the tube and the mixture incubated for 3 h more with gentle shaking (70 rpm), after which the cells were

harvested (1500 × *g*, 10 min, 24 °C), resuspended in 1 M sorbitol (300 µL) and spread on Selection-I medium. After drying for 5 min, a top agar layer of Selection-I medium was overlaid on the cells. The plates were incubated at 30 °C in a 12 h light-dark cycle for four days until colonies appeared between the agar layers. The colonies were extracted from the agar, suspended in 1 M sorbitol, and spotted on Selection-II medium. For subsequent rounds of propagation, cells were scraped from the surface of the agar, resuspended in 1 M sorbitol, and spotted on Selection-III medium. The yeast/cyanobacteria chimeras are sensitive to high constant light and are propagated under 12 h light-dark cycle light dark cycles with light intensity of 50 $\mu E/m^2 \cdot s$.

Cell count of *S. cerevisiae* cox2-60/cyanobacteria chimeras

Agar disks containing cells on Selection III medium were extracted manually from the agar plate and placed inside a microcentrifuge tube. Sorbitol (1 M, 200 µL) was added to the surface of the agar and pipetted to make a cell suspension. The tube was centrifuged for 5 s to remove the cell suspension from the agar. The suspension was added to a reusable glass slide and counted in triplicate from a brightfield image using the Countess II FL Automated Cell Counter (Fisher cat. # AMQAF1000) per the manufacturer's instructions.

Microscopic sample preparation of yeast/cyanobacteria chimeras

Chimeric cells are washed and resuspended in 1 M sorbitol to a high density. These cells were analyzed using total internal reflection fluorescence microscopy (TIRF) on a custom-built microscope with a Zeiss Axiovert 200 M stand[23]. A Cobolt diode-pumped 561 nm laser was used to excite phycobilins and normal bright field images were always captured chimera cells. The pTIRF images were acquired with a Photometric 512 Evolve EMCCD camera. Samples were viewed and imaged using a 100x oil immersion objective lens with NA = 1.4. All images were processed with ImageJ 1.53cto overlay qTIRF image and a brightfield image acquired from the same sample position. For analysis of yeast/cyanobacteria chimeras using fluorescence confocal microscopy, the chimeric cells were washed from plate spots using Hank's Buffered Salt Solution (HBSS; NaCl (140 mM), KCl (5 mM), $CaCl_2$ (1 mM), $MgSO_4$ heptahydrate (0.4 mM), $MgCl_2$ hexahydrate (0.5 mM), Na_2PO_4 dihydrate (0.3 mM), KH_2PO_4 (0.4 mM), D-glucose (6 mM), $NaHCO_3$ (4 mM)). The cells were resuspended in 50 µL HBSS with 1X ConA (40X Concanavalin A Stock solutions (40X); Thermo Fisher C827 was dissolved in sodium bicarbonate 0.1 M and HBSS). The cells were then incubated 37 °C for 10 min in the dark. The cells are centrifuged at 1500 × *g* and washed twice with HBSS. The ConA-stained cells were incubated with 50 µL HBSS with 37% paraformaldehyde for 1 hour in a nutator in dark. Samples were analyzed with a commercial Leica SP8 fluorescence confocal microscope. Samples were viewed and imaged through a 63X/1.40 HC PL APO Oil CS2 lens and excited with 488 nm and 561 nm laser. Emission wavelengths in the 510-530 nm range were detected with photomultiplier tube (PMT) detector, and emission wavelengths in the 616-650 range were detected using a high-sensitivity GaAsP HyD detector. Leica Application Suite (LASX) was used to collect raw data. All images were processed with ImageJ 1.53c to overlay the two channels.

Scanning transmission electron microscope sample preparation

The control and chimera cells were pelleted by centrifugation (6000 × *g*, 5 min). The supernatant was resuspended in fixative (2.5% EM-grade glutaraldehyde and 2.0% EM-grade formaldehyde in 0.1 M sodium cacodylate buffer, pH 7.4) for overnight at 4 °C. The fixative was then removed, replaced briefly with buffer, and then replaced with 1% osmium tetroxide in buffer for 90 min in dark. Each sample was then subjected to 10 min buffer rinse, after which it was placed in 1% aqueous uranyl acetate and left overnight. The next day, samples were dehydrated via a graded ethanol series, culminating in propylene oxide. Following a graded propylene oxide; Epon812 series, the nuclear pellets were embedded in Epon812 prior to cutting. Ultrathin (ca. 90 nm) Epon sections on grids were stained with 1% aqueous uranyl acetate and Reynold's Lead Citrate solution. After the grids dried, areas of interest were imaged at 160 kV, spot 3 using a Philips/FEI (now Thermo Fisher FEI) Tecnai G2 F20 S-TWIN transmission electron microscope in the Microscopy Suite at the Beckman Institute of Advanced Science and Technology (University of Illinois at Urbana-Champaign).

Reporting summary

Further information on research design is available in the Nature Portfolio Reporting Summary linked to this article.

Data availability

NCBI accession CAE46506.1 [https://www.ncbi.nlm.nih.gov/protein/CAE46506.1], XP_005536231.1 [https://www.ncbi.nlm.nih.gov/protein/XP_005536231.1], KAF6002099.1 [https://www.ncbi.nlm.nih.gov/protein/KAF6002099.1], PXF48205.1 [https://www.ncbi.nlm.nih.gov/protein/PXF48205.1], XP_005707402.1 [https://www.ncbi.nlm.nih.gov/protein/XP_005707402.1], CAX16542.1 [https://www.ncbi.nlm.nih.gov/protein/CAX16542.1], TRINITY_DN12309 [https://www.ncbi.nlm.nih.gov/protein/CAX16542.1/], NP_178146.1 [https://www.ncbi.nlm.nih.gov/protein/NP_178146.1], and NC_003076.8 [https://www.ncbi.nlm.nih.gov/nuccore/NC_003076.7], as well as UniProt accession M1V528, Q39002, and Q6MEM5 were used in this study. Source data are provided with this paper.

References

1. Mereschkowsky, C. Uber natur und ursprung der chromatophoren im pflanzenreiche. *Biologisches Centralblatt* **25**, 293–604 (1905).
2. Margulis, L. *Origin of Eukaryotic Cells: Evidence and Research Implications for a Theory of the Origin and Evolution of Microbial, Plant and Animal Cells on the Precambrian Earth*. (Yale University Press, 1970).
3. Zimorski, V., Ku, C., Martin, W. F. & Gould, S. B. Endosymbiotic theory for organelle origins. *Curr. Opin. Microbiol.* **22**, 38–48 (2014).
4. Jensen, P. E. & Leister, D. Chloroplast evolution, structure and functions. *F1000prime reports* vol. 6 (2014).
5. Martin, W. & Kowallik, K. V. Annotated english translation of Mereschkowsky's 1905 paper 'über natur und ursprung der chromatophoren im pflanzenreiche'. *Eur. J. Phycol.* **34**, 287–295 (1999).
6. Raven, J. A. & Allen, J. F. Genomics and chloroplast evolution: what did cyanobacteria do for plants? *Genome Biol.* **4**, 209 (2003).
7. Allen, J. F., Raven, J. A. & Allen, J. F. The function of genomes in bioenergetic organelles. *Philos. Trans. R. Soc. Lond. B. Biol. Sci.* **358**, 19–38 (2003).
8. Greub, G. & Raoult, D. History of the ADP/ATP-translocase-encoding gene, a parasitism gene transferred from a Chlamydiales ancestor to plants 1 billion years ago. *Appl. Environ. Microbiol.* **69**, 5530–5535 (2003).
9. Amiri, H., Karlberg, O. & Andersson, S. G. E. Deep origin of plastid/parasite ATP/ADP translocases. *J. Mol. Evol.* **56**, 137–150 (2003).
10. Major, P., Embley, T. M. & Williams, T. A. Phylogenetic diversity of NTT nucleotide transport proteins in free-living and parasitic bacteria and eukaryotes. *Genome Biol. Evol.* **9**, 480–487 (2017).
11. Ast, M. et al. Diatom plastids depend on nucleotide import from the cytosol. *Proc. Natl Acad. Sci. USA* **106**, 3621–3626 (2009).
12. Klingenberg, M. Molecular aspects of the adenine nucleotide carrier from mitochondria. *Arch. Biochem. Biophys.* **270**, 1–14 (1989).
13. Voon, C. P. & Lim, B. L. ATP translocation and chloroplast biology. *Natl Sci. Rev.* **6**, 1073–1076 (2019).
14. Haferkamp, I., Fernie, A. R. & Neuhaus, H. E. Adenine nucleotide transport in plants: much more than a mitochondrial issue. *Trends Plant Sci.* **16**, 507–515 (2011).

15. Gurgel, C. F. D. & Lopez-Bautista, J. Red algae. *Encycl. Life Sci*. https://repository.si.edu/bitstream/handle/10088/11430/sms_gurgel_2007.pdf (2007).
16. Sheath, R. G. & Vis, M. L. Red algae. in *Freshwater Algae of North America* 237–264 (Elsevier, 2015).
17. Strassert, J. F., Irisarri, I., Williams, T. A. & Burki, F. A molecular timescale for eukaryote evolution with implications for the origin of red algal-derived plastids. *Nat. Commun.* **12**, 1879 (2021).
18. Janouškovec, J. et al. Evolution of red algal plastid genomes: ancient architectures, introns, horizontal gene transfer, and taxonomic utility of plastid markers. *PloS One* **8**, e59001 (2013).
19. Löffelhardt, W. & Bohnert, H. *The Cyanelle (Muroplast) Of Cyanophora Paradoxa: A Paradigm For Endosymbiotic Organelle Evolution*. in *Symbiosis: Mechanisms and Model Systems* 111–130 (Springer, 2001).
20. Steiner, J. M. & Löffelhardt, W. *The Photosynthetic Apparatus Of The Living Fossil, Cyanophora Paradoxa. Bioenerg. Process. Cyanobacteria Evol. Singul. Ecol. Divers*. 71–87 (2011).
21. Figueroa-Martinez, F., Jackson, C. & Reyes-Prieto, A. Plastid genomes from diverse glaucophyte genera reveal a largely conserved gene content and limited architectural diversity. *Genome Biol. Evol.* **11**, 174–188 (2019).
22. Jackson, C., Clayden, S. & Reyes-Prieto, A. The Glaucophyta: the blue-green plants in a nutshell. *Acta Soc. Bot. Pol*. **84**, 149–165 (2015).
23. Cournoyer, J. E. et al. Engineering artificial photosynthetic lifeforms through endosymbiosis. *Nat. Commun.* **13**, 2254 (2022).
24. Ornelas, M. Y., Cournoyer, J. E., Bram, S. & Mehta, A. P. Evolution and synthetic biology. *Curr. Opin. Microbiol.* **76**, 102394 (2023).
25. Gao, Y. et al. Introducing carbon assimilation in yeasts using photosynthetic directed endosymbiosis. *Nat. Commun.* **15**, 5947 (2024).
26. Zrenner, R., Stitt, M., Sonnewald, U. & Boldt, R. Pyrimidine and purine biosynthesis and degradation in plants. *Annu. Rev. Plant Biol.* **57**, 805–836 (2006).
27. Walker, J. E. & Runswick, M. J. The mitochondrial transport protein superfamily. *J. Bioenerg. Biomembr.* **25**, 435–446 (1993).
28. Winkler, H. H. & Neuhaus, H. E. Non-mitochondrial ATP transport. *Trends Biochem. Sci.* **24**, 64–68 (1999).
29. Schmitz-Esser, S. et al. ATP/ADP translocases: a common feature of obligate intracellular amoebal symbionts related to Chlamydiae and Rickettsiae. *J. Bacteriol.* **186**, 683–691 (2004).
30. Mehta, A. P. et al. Engineering yeast endosymbionts as a step toward the evolution of mitochondria. *Proc. Natl Acad. Sci. USA* **115**, 11796–11801 (2018).
31. Atkinson, H. J., Morris, J. H., Ferrin, T. E. & Babbitt, P. C. Using sequence similarity networks for visualization of relationships across diverse protein superfamilies. *PloS One* **4**, e4345 (2009).
32. Gerlt, J. A. et al. Enzyme function initiative-enzyme similarity tool (EFI-EST): a web tool for generating protein sequence similarity networks. *Biochim. Biophys. Acta* **1854**, 1019–1037 (2015).
33. Shannon, P. et al. Cytoscape: a software environment for integrated models of biomolecular interaction networks. *Genome Res* **13**, 2498–2504 (2003).
34. Moustafa, A., Reyes-Prieto, A. & Bhattacharya, D. Chlamydiae has contributed at least 55 genes to Plantae with predominantly plastid functions. *PloS One* **3**, e2205 (2008).
35. Price, D. C. et al. Analysis of an improved Cyanophora paradoxa genome assembly. *DNA Res* **26**, 287–299 (2019).
36. Ponce-Toledo, R. I. et al. An early-branching freshwater cyanobacterium at the origin of plastids. *Curr. Biol.* **27**, 386–391 (2017).
37. Thuswaldner, S. et al. Identification, expression, and functional analyses of a thylakoid ATP/ADP carrier from Arabidopsis. *J. Biol. Chem.* **282**, 8848–8859 (2007).
38. Mehta, A. P. et al. Toward a synthetic yeast endosymbiont with a minimal genome. *J. Am. Chem. Soc.* **141**, 13799–13802 (2019).
39. Linka, N. et al. Phylogenetic relationships of non-mitochondrial nucleotide transport proteins in bacteria and eukaryotes. *Gene* **306**, 27–35 (2003).
40. Letunic, I. & Bork, P. Interactive Tree Of Life (iTOL) v5: an online tool for phylogenetic tree display and annotation. *Nucleic Acids Res.* **49**, W293–W296 (2021).

Acknowledgements

The research reported in this publication was supported by the National Institute of General Medical Sciences of the National Institutes of Health under Award Number R01GM139949. This funding was received by A.P.M. The content is solely the responsibility of the authors and does not necessarily represent the official views of the National Institutes of Health. A.P.M. also thanks funding from Moore–Simons Project on the Origin of the Eukaryotic Cell, GBMF9732, grant https://doi.org/10.37807/GBMF9732.

Author contributions

A.P.M., B.C.D. designed experiments. B.C.D., J.E.C., Y.G., C.L.W., S.B. performed biochemical experiments, microscopy experiments and obtained all data reported in this manuscript. A.P.M., B.C.D. analyzed the data. All the authors helped with manuscript preparation.

Competing interests

Authors declare that they have no competing interests.

Additional information

Supplementary information The online version contains supplementary material available at https://doi.org/10.1038/s41467-024-54051-1.

Correspondence and requests for materials should be addressed to Angad P. Mehta.

Peer review information : *Nature Communications* thanks the anonymous reviewers for their contribution to the peer review of this work. A peer review file is available.